ISBN: 978-3-95450-208-0 doi:10.18429/JACoW-IPAC2019-THPRB083

DETAILED ANALYSIS OF THE BASELINE DOSE LEVELS AND LOCALIZED RADIATION SPIKES IN THE ARC SECTIONS OF THE LARGE HADRON COLLIDER DURING RUN 2

Kacper Biłko*, Markus Brugger, Rubén García Alía, Fiona Harden†, Yacine Kadi, Oliver Stein
CERN, Geneva, Switzerland

Abstract

The Large Hadron Collider (LHC) has eight insertion regions (IRs) which house the large experiments or accelerator equipment. These IRs are interconnected with the arc sections consisting of a periodic magnet structure. During the operation of the LHC small amounts of the beam particles are lost, creating prompt radiation fields in the accelerator tunnels and the adjacent caverns. One of the main loss mechanisms in the LHC arc sections is the interaction of the beam particles with the residual gas molecules. The analysis of the dose levels based on the beam loss measurement data shows that the majority of the measurements have similar levels, which allow to define baseline values for each arc section. The baseline levels decreased during the years 2015, 2016 and stabilised in 2017 and 2018 at annual dose levels below 50 mGy, which can be correlated with the residual gas densities in the LHC arcs. In some location of the arcs radiation spikes exceed the base line by more than two orders of magnitude. In addition to the analysis of these dose levels a novel approach of identifying local dose maxima and the main driving mechanisms creating these radiation spikes will be presented.

INTRODUCTION

The Large Hadron Collider (LHC) at the European Organization for Nuclear Research (CERN) is a circular collider with a total circumference of almost 27 km, where two coplanar particle beams are accelerated and, in the centres of the four large experiments (ALTAS, ALICE, CMS and LHCb), collided [1]. Its operation leads to small but continuous beam losses, that result in mixed field radiation. Therefore, electronic equipment located close to the accelerator might be affected through both single event effects (SEEs) and cumulative effects, i.e. displacement damages and Total Ionising Dose (TID). Consequently, the equipment failures may induce the interruption of the LHC operation, thus decreasing overall accelerator performance.

LHC Layout

The experiments are located in the 4 Long Straight Sections (LSSs). In total LHC contains 8 LSSs, where remaining 4 constitute essential accelerator systems (collimators, radio-frequency cavities or beam dump). The LSS are enclosed by Dispersion Suppressor (DS) sections. Together they form the Insertion Regions (IRs). The IRs are interconnected with the arc sections where the magnets are periodically arranged and the beam is being bent and focused. In the LHC it is accomplished using a FODO structure consisting of focusing quadrupole magnet followed by three bending dipole magnets, defocusing quadrupole and another three bending magnets. A schematic structure is illustrated in Fig. 1.

The LHC is organized in small subsections that are called half-cells. The arc section starts in the 12th half-cell of an IR and ends in the 12th half-cell of the next IR [2], e.g. *arc 45* spans between two DSs: the right of IR 4 and the left of IR 5. An arc half-cell contains the half of the FODO cell.

Main Beam Loss Mechanisms

Various beam loss mechanisms are present during the beam's circulation in the LHC. With the focus on the continuous losses, the major expected one can be determined, depending on the location in the accelerator. In the experimental IRs collision debris is produced as a result of particle interactions. It has strong forward momentum, resulting in high radiation levels downstream of the experiments [3]. These losses scale with the luminosity of the nearby experiment. In order to protect the machine from deviating particles, dedicated collimation regions are inserted to stop the particles which exceed the acceptance of the LHC. Particles with too large betatron oscillations are stopped in IR7 and particles with a too large energy deviation are stopped in IR3. The analysis showed that under the same operational conditions, these losses scale with the integrated beams intensity. This paper focuses on the arc sectors, where the dominating expected beam loss mechanism is the scattering of the beam on residual gas molecules in the vacuum chamber. With the same operational conditions these losses scale with the residual gas density, which is considered to be constant along the arc section, and integrated beam intensity.

TID Monitoring in the LHC

The beam loss monitoring system was developed at CERN to prevent the damages of accelerator components and magnet quenches. It consists of more than 3600 Beam Loss Monitors (BLMs), i.e. ionisation chambers filled with nitrogen gas, distributed around the LHC in the critical locations [4]. Thanks to the exact calibration of the BLMs, through the dedicated processing [5], this system can be additionally used for TID measurements. In the arc sections the installation pattern of the BLMs reflects the periodic magnet arrange-

* kacper.bilko@cern.ch
† Presenter

Content from this work may be used under the terms of the CC BY 3.0 licence (© 2019). Any distribution of this work must maintain attribution to the author(s), title of the work, publisher, and DOI

ISBN: 978-3-95450-208-0 doi:10.18429/JACoW-IPAC2019-THPRB083

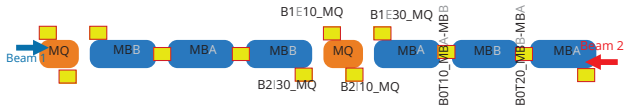

Figure 1: Schematic representation of the LHC ARC FODO cell with the BLMs locations (yellow rectangles). MQ denotes quadrupole magnets whereas MB(B/A) dipole ones. There are six different locations (BLM families) of BLMs with respect to the half-cell: 4 in the beams plane (B1_10, B1_30, B2_10, B2_30) and 2 on top of the interconnection between dipole magnets (B0T10, B0T20). Grey colour letters vary depending on the half-cell.

ment. As presented in Fig. 1, each ARC half-cell contains 6 BLMs at different locations which are periodically repeated.

DOSE LEVELS IN THE ARC SECTIONS

We carried out a detailed analysis of the TID levels during the proton-proton (p-p) operation in the arc sections of the LHC. It was confirmed that both the dose level and time evolution for majority of the monitors within one BLM family were similar. Based on this fact we defined the *baseline* dose level as an averaged TID within one BLM family in the arc sector caused by the interactions of the beams with residual gas. Losses for the baseline BLMs scale with both residual gas density and time integrated beam intensity.

Nonetheless, unexpectedly in some locations the dose levels exceeded the baseline by more than two orders of magnitude. For these *spikes*, the major beam loss mechanism was not anymore the beam-gas interaction. The causes are being studied in detail. In most cases they are brought about as a result of the luminosity production in the experiments.

Typical Levels

The detailed studies showed that the annual baseline TID levels for the p-p operation are low, i.e. below 100 mGy (Gy in nitrogen). In Run 2 the maximum values (among BLM families and arc sectors) of annual baseline TIDs were following: 2015 – 77 mGy, 2016 – 99 mGy, 2017 – 49 mGy, 2018 – 34 mGy. The levels normalised with the integrated beams intensity were decreasing in the years 2015-2017 and remained similar in 2018 (for all arc sections apart from 12). Moreover, the levels in 2018 were comparable among all the arc sections for a given BLM family. We analysed not only annual TID baseline levels but also their evolution. An example of such is depicted in Fig. 2. For all arc sectors, until the mid-2017, a nonlinear behaviour can be observed, which would have not been the case if the residual gas density had been constant. Since the slope of the trace was decreasing, residual gas density had to decrease as well. Provided that interaction with the residual gas was the major beam loss mechanism, it can be concluded that a conditioned state of vacuum has been achieved in late 2017.

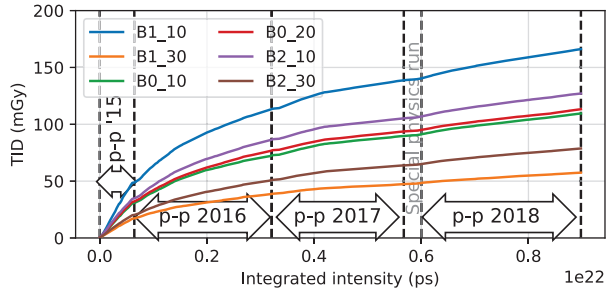

Figure 2: An example of the baseline TID level evolution (obtained as a non-spike TID averaged over one BLM family [5]) in Run 2 for the arc section 45. The evolution and dose levels are comparable for all arc sections.

Critical Locations

The least radiation tolerant electronics presently installed in the LHC arcs has an estimated annual TID budget of a few tens of Gy, which is well above the baseline dose levels. However, the analysis showed that in the spike locations the TIDs can get close to the radiation budget. Therefore, it is critical to detect all the anomaly locations where the radiation is higher than expected. Based on the distribution of annual TIDs we selected the spike candidates [5]. In Run 2 in some locations the baseline dose levels were exceeded by more than two orders of magnitude, e.g. as presented in Fig. 3 for the arc sector 45. In this arc the majority of spikes appeared in beam 2, that is outgoing from the experiment located at IR5, and could be observed only during collisions.

Most of the spikes show dynamic behaviour, vanishing or appearing from year to year. The detection based on the annual TIDs is not sufficient in terms of effective prevention of radiation induced failures, thus the new algorithm of the evolution analysis has been developed. TID evolution for each spike candidate was compared with the baseline evolution for the respective BLM family. Discrepancies between both evolutions indicate time period of the anomaly occurrence. Applying the filtering by the beam mode [6] it was possible to retrieve evolution for specific accelerator state, e.g. collisions. Comparing the baseline evolution with the spike evolution allows to narrow down the set of accelerator settings that could drive the spike. Evolution analysis follows the LHC operation on the daily basis, enabling the discrepancies detection just after their occurrence. Consequently, if necessary, the mitigation interventions can be planned and performed more efficiently.

An insight of the spikes dynamics is presented in Fig. 4. The TID evolution for spikes in the half-cells: 23R4, 29R4 and 33L5 was separated for beam modes that involve beam collisions and the ones that do not. All of them are related to the same BLM family – beam 2, position 30. The discrepancies between the spike and corresponding baseline evolutions can be observed only for collision beam modes, indicating that the spikes are caused by change of machine settings needed for collisions or by collisions themselves (particle debris). In 2015 none of these spikes were ob-

Content from this work may be used under the terms of the CC BY 3.0 licence (© 2019). Any distribution of this work must maintain attribution to the author(s), title of the work, publisher, and DOI

ISBN: 978-3-95450-208-0 doi:10.18429/JACoW-IPAC2019-THPRB083

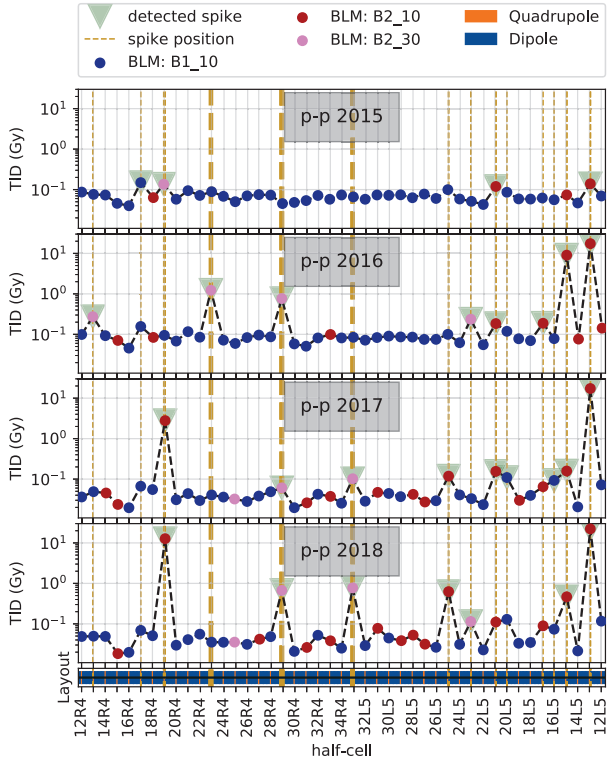

Figure 3: Annual dose levels in the Run 2, in the arc section 45. In each half-cell only side BLM with the highest TID is plotted.

served. Then, in 2016 two of them – 23R4, 29R4 appeared, but their evolution was not analogous. The growth of the spike in the half-cell 23R4 decreased since the beginning of September 2016, as opposed to the spike in the half-cell 29R4. In 2017 the spike in the half-cell 23R4 vanished, however new one appeared in the half-cell 33L5. Afterwards in 2018, losses for both spikes (29R4, 33L5) increased with respect to the year 2017.

In the years 2015, 2016 and 2018, the LHC was operated also with Pb ions but the runs were shorter (about 15% of an annual beam present-time) and the intensities were reduced (approximately by 4 orders of magnitude [2]). Therefore as expected, the baseline TID levels were lower with respect to the p-p operation. However, the spike pattern was different and just a couple of them appeared in the same locations as during p-p operation. Only in a few cases spikes exceeded TID levels of 1 Gy in 2015 and 2016. The ion run 2018 brought some new anomalies. We identified position-wise symmetric spikes at both sides of the ALICE experiment (IR 2), in the half-cells: 16,14 and 12; with the TIDs up to 44 Gy. They occurred only in the experiment's outgoing beams. Additionally, some spikes arose in the half-cells: 18L3, 13L5, 13R7, 16R8; having the TID ranging from 3 to 6 Gy. Despite shorter operation, the TIDs for these spikes exceeded the TID levels of the p-p 2018 operation at these positions by up to a factor 100. These levels imply increased risk of radiation damages in the nearby electronics.

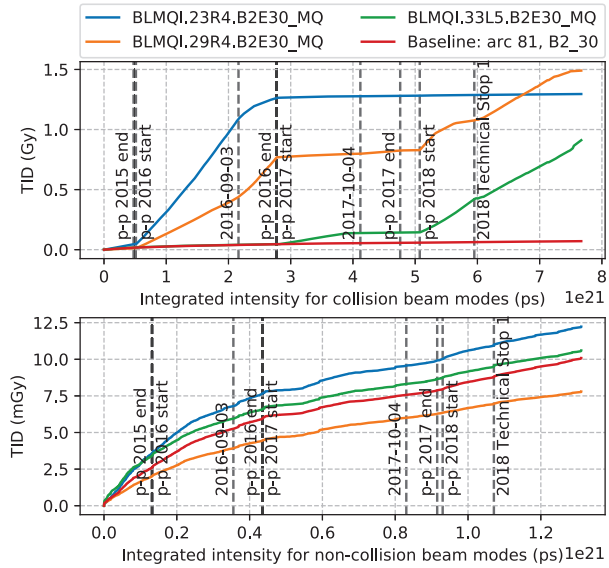

Figure 4: TID evolution over integrated beam intensity for spikes in half-cells: 23R4, 29R4 and 33L5. The evolution has been split into two traces – first involving only collision beam modes, second involving the rest of beam modes.

The majority of the spikes in Run 2 occurred when the beams were collided, hence the discrepancies with baseline can be observed only for collision beam modes. Furthermore, the evolution might be spilt into each of beam modes, narrowing the candidates for the causes. It is also possible to classify spikes into groups that shares similar behaviour, hence to find correlations and symmetries in the LHC loss patterns.

CONCLUSION

We performed a comprehensive analysis of the TID levels in the arc sections of the LHC. The baseline TID levels were low, and in terms of TID damages, they were not dangerous for arc electronics. However, the localised anomalies can exceed the baseline TIDs by more than two orders of magnitude. The dynamism of their evolution implies that continuous monitoring is critical. The developed algorithm of the spikes analysis provides a powerful tool not only for the spikes detection and monitoring, but also for the cause studies. Through the comparison of the spike with the respective baseline evolution the investigations are unbiased by the accelerator parameters that affected losses in general, and therefore the focus can be only on the spike itself. Some LHC ARC half-cells are equipped with the dedicated radiation monitors (RadMons). Before Run 3, we plan to integrate them into the real-time radiation monitoring, that together with FLUKA simulations, will enable dose evaluation at equipment locations. Therefore, the preventive maintenance will be easily anticipated, resulting in an improvement of the LHC availability.

Content from this work may be used under the terms of the CC BY 3.0 licence (© 2019). Any distribution of this work must maintain attribution to the author(s), title of the work, publisher, and DOI

ISBN: 978-3-95450-208-0 doi:10.18429/JACoW-IPAC2019-THPRB083

Content from this work may be used under the terms of the CC BY 3.0 licence (© 2019). Any distribution of this work must maintain attribution to the author(s), title of the work, publisher, and DOI

REFERENCES

[1] L. Evans and P. Bryant, "LHC Machine," JINST **3** (2008) S08001. doi:10.1088/1748-0221/3/08/S08001

[2] O. S. Bruning, P. Collier, P. Lebrun, S. Myers, R. Ostojic, J. Poole and P. Proudlock, "LHC Design Report Vol.1: The LHC Main Ring," doi:10.5170/CERN-2004-003-V-1

[3] R. García Alía *et al.*, "LHC and HL-LHC: Present and Future Radiation Environment in the High-Luminosity Collision Points and RHA Implications," IEEE Trans. Nucl. Sci. **65** (2018) no. 1, p. 448. doi:10.1109/TNS.2017.2776107

[4] E. B. Holzer *et al.*, "Beam Loss Monitoring for LHC Machine Protection," Phys. Procedia **37** (2012) p. 2055. doi:10.1016/j.phpro.2012.04.110

[5] K. Bilko, O. Stein, K. Malarz ,"Detailed analysis of the evolution and distribution of the total ionising dose in the LHC arc sections during the accelerator operation", CERN, Switzerland, CERN-THESIS-2018-307, 2018. http://cds.cern.ch/record/2652979

[6] R. Alemany, M. Lamont, and S. Page. "Functional Specification LHC Modes", CERN, Switzerland, Tech. Rep. LHC-OP-ES-0005 rev 1.1, 2009, https://edms.cern.ch/ui/file/865811/1.1/LHC-OP-ES-0005-10-10.pdf